ELSEVIER

Journal of Neuroscience Methods 168 (2008) 494–499

JOURNAL OF NEUROSCIENCE METHODS

www.elsevier.com/locate/jneumeth

Short communication

Assessing transient cross-frequency coupling in EEG data

Michael X Cohen *

Department of Epileptology and Center for Life and Brain, University of Bonn, Germany

Received 22 September 2007; received in revised form 23 October 2007; accepted 23 October 2007

Abstract

Synchronization of oscillatory EEG signals across different frequency bands is receiving waxing interest in cognitive neuroscience and neurophysiology, and cross-frequency coupling is being increasingly linked to cognitive and perceptual processes. Several methods exist to examine cross-frequency coupling, although each has its limitations, typically by being flexible only over time or over frequency. Here, a method for assessing transient cross-frequency coupling is presented, which allows one to test for the presence of multiple, dynamic, and flexible cross-frequency coupling structure over both time and frequency. The method is applied to intracranial EEG data, and strong coupling between gamma (~40–80 Hz) and upper theta (~7–9 Hz) was observed. This method might have useful applications in uncovering the electrophysiological correlates of cognitive processes.

Keywords: Oscillations; Cross-frequency coupling; Phase coupling; Gamma; Intracranial EEG

Electrophysiological brain oscillations in multiple frequency bands, ranging from delta (1–4 Hz) to gamma (up to 150 Hz) and beyond, have been linked to a range of cognitive and perceptual processes (Varela et al., 2001; Steriade, 2006). Although in principle oscillations in different frequency bands may act independently, statistical relations among activities in different frequency bands have been reported. Such "cross-frequency coupling" has been observed in several brain regions including the hippocampus, prefrontal cortex, and sensory cortex (Chrobak and Buzsaki, 1998; Buzsaki and Draguhn, 2004; Jones and Wilson, 2005; Lakatos et al., 2005; Mormann et al., 2005; Canolty et al., 2006; Jensen and Colgin, 2007). It is thought to reflect coherent neural communication and information encoding (Lisman, 2005; Jensen and Colgin, 2007), and has been hypothesized to support processes including perceptual binding, spatial and temporal memory encoding, and information processing (Lisman, 2005).

There are several manifestations of cross-frequency coupling in the brain, and different methods have been developed to identify different types of coupling. For example, one type of coupling is called phase–amplitude coupling, and refers to a synchronization of oscillation power fluctuations with the phase of a slower oscillation. For example, in the entorhinal and prefrontal cortices, the amplitude of gamma oscillations (~30–80 Hz or sometimes up to 150 Hz) increases during specific phases of theta (4–8 Hz) (Chrobak and Buzsaki, 1998; Canolty et al., 2006; Demiralp et al., 2007). Although these and other related methods (Bruns et al., 2000; Schack et al., 2005) are sensitive to changes in cross-frequency coupling over time, one disadvantage is that the researcher must specify *a priori* the frequency bands at which synchronization will be assessed. Other methods have been presented that allow a more data-driven approach, i.e., by calculating phase–amplitude synchronization indices between multiple frequency bands (e.g., power from oscillations ranging from 20 to 200 Hz and phase from oscillations ranging from 2 to 20 Hz). These synchronization indices can then be plotted in amplitude–phase space, and regions of phase–amplitude synchronization can be visually or statistically identified and interrogated for further analysis (Canolty et al., 2006). One disadvantage of this approach, however, is that the temporal dynamics of cross-frequency coupling are lost. That is, this method is not robust to dynamic or transient changes in cross-frequency coupling over time and/or frequency. Another method is termed "n:m" phase synchronization, and involves examining the synchrony between phase values at one frequency band and phase values at an integer multiple of that frequency band (Tass et al., 1998; Palva et al., 2005; Schack and Weiss, 2005).

* Correspondence address: Department of NeuroCognition, University of Bonn, Sigmund-Freud-Street 25, Bonn 53105, Germany.
Tel.: +49 228 2871 9345.
E-mail address: mikexcohen@gmail.com.

0165-0270/$ – see front matter © 2007 Elsevier B.V. All rights reserved.
doi:10.1016/j.jneumeth.2007.10.012

This method is useful for examining amplitude-independent phase-locking, but is limited to coupling among integer-multiple frequency bands (e.g., 10, 20, 40 Hz). Thus, different measures of cross-frequency coupling are suited for different purposes. To date, no cross-frequency coupling method exists that is flexible in both time and frequency. Here I present a novel method for statistically assessing the extent to which fluctuations in the power of one frequency band are synchronized with activity in a lower frequency band. This method requires no *a priori* assumptions about which frequency bands should be synchronized, but rather relies on the natural statistical properties of the data to reveal cross-frequency synchronization. It is sensitive to transient changes in cross-frequency coupling over both time and frequency, can simultaneously assess multiple cross-frequency synchronizations (i.e., different synchronizations in different frequency bands), and therefore might be well-suited to investigating possible cross-frequency coupling during dynamic and/or brief cognitive or perceptual events. Further, the method produces synchronization indices that can be statistically assessed over time, trials, experimental conditions, and subjects. This approach might be especially useful for exploratory analyses, although it is also appropriate for hypothesis-driven tests.

1. Dataset

The data analyzed here were taken from a patient (female, aged 37 years) with electrodes implanted for pre-surgical evaluation of epilepsy. Electrode placement was made on clinical grounds. The electrode used here was in a 4×8 grid placed over left lateral temporal cortex; the electrode used is located in the posterior superior temporal gyrus. During the recording, the patient watched a 4-s video clip of two solid circles moving on the screen. The task was to pay attention and to judge, on a scale of 1–4, how subjectively quickly the circles were moving. The patient was seizure-free during the recordings and for the previous 24 h, and visual inspection revealed no artifacts or anomalies in the segment of data used here. EEG data were sampled at 1 kHz and referenced to linked mastoids.

2. Brief overview of method

The idea behind this approach is that if the power of oscillations at a high frequency are synchronized with a slower frequency oscillation, the upper frequency power time series will itself oscillate at that lower frequency (Bruns et al., 2000). Here, an empirical approach is used to select the lower frequency band based on the observed fluctuations in the upper power time series, and standard phase coherence measures are used to evaluate the phase synchronization between the upper frequency power time series and the lower frequency EEG oscillation.

3. Details of method

All analyses were conducted in Matlab 6.5 using the signal processing and eeglab toolboxes, the latter of which is free to download (Delorme and Makeig, 2004), and supplemented by code written by the author. Sample Matlab code for conducting this analysis is available from the author upon request. This method utilizes a three-step plan, which is repeated over many time–frequency windows. Here, windows of 400 ms and 5 Hz were used; in the following example I use one of many windows to illustrate the analysis.

In the first step, the upper frequency power time series is extracted from a window (e.g., 400 ms) of the raw EEG data. The power time series reflects time-changing fluctuations in the amount of energy at that specific frequency band. This was done by narrow band-pass filtering in combination with the Hilbert transform. For example, EEG data were band-pass filtered from 73.5 to 78.5 Hz (Fig. 1A and B), and then the power time series was extracted as the squared magnitude of $z(t)$, the analytic signal obtained from the Hilbert transform (power time series: $p(t) = \text{real}[z(t)]^2 + \text{imag}[z(t)]^2$) (Fig. 1C). Filtering should be done on a sufficiently long time series of EEG data to prevent edge-effect artifacts from clouding the results. Here, filtering was done on 2000 ms extra data on either side of the selected window; visual inspection confirmed that edge effects were not present in the window of interest. The filter utilizes a two-way, least-squares FIR procedure (as implemented in the eegfilt.m script included in the eeglab package; Delorme and Makeig, 2004). This filtering method uses a zero-phase forward and reverse operation (Mitra, 2001), which ensures that phase values are not distorted, as can occur with forward-only filtering methods. After filtering, data segments were cut back to the 400 ms window of interest (displayed in Fig. 1). This method of band pass filtering and the Hilbert transform provides analogous results to a complex wavelet transform (Le Van Quyen et al., 2001; Quian Quiroga et al., 2002; Bruns, 2004).

In the second step, a lower frequency band that the upper frequency power time series might be synchronized with is empirically identified. This works by first computing the FFT of the upper frequency power time series in a specific time window. The goal of this step is to identify rhythmic fluctuations in the upper frequency power time series; if the upper frequency power time series is synchronized with a lower frequency oscillation, the power time series will not be constant over time, but instead will fluctuate at the lower oscillation frequency. For example, if 75 Hz oscillations are synchronized with a 7.5 Hz oscillation (i.e., upper theta), the power time series of the 75 Hz oscillation might itself oscillate at 7.5 Hz. In this case, the FFT of the 75 Hz power time series will produce a spike at 7.5 Hz (Fig. 1D). The width of the time window is not trivial, because it defines the lower frequency limit of the lower synchronizing oscillation. For example, if a window of 300 ms is used at a sampling rate of 1 kHz, the lower synchronization frequency should have a periodicity of at least 150 ms (6.6 Hz) (i.e., at least two oscillation cycles with which to measure phase synchrony). Intuitively, larger time windows improve the frequency resolution of the lower oscillation at the expense of temporal precision of cross-frequency coupling, and *vice versa*. Here, a time window of 400 ms is used, which means frequencies above 5 Hz will be identified (given the two-cycle criterion). Next, the peak of the FFT is identified. Identification is constrained at the lower end as described, and at the upper end by the upper frequency (in this example, 75 Hz). The upper limit could also be constrained by an

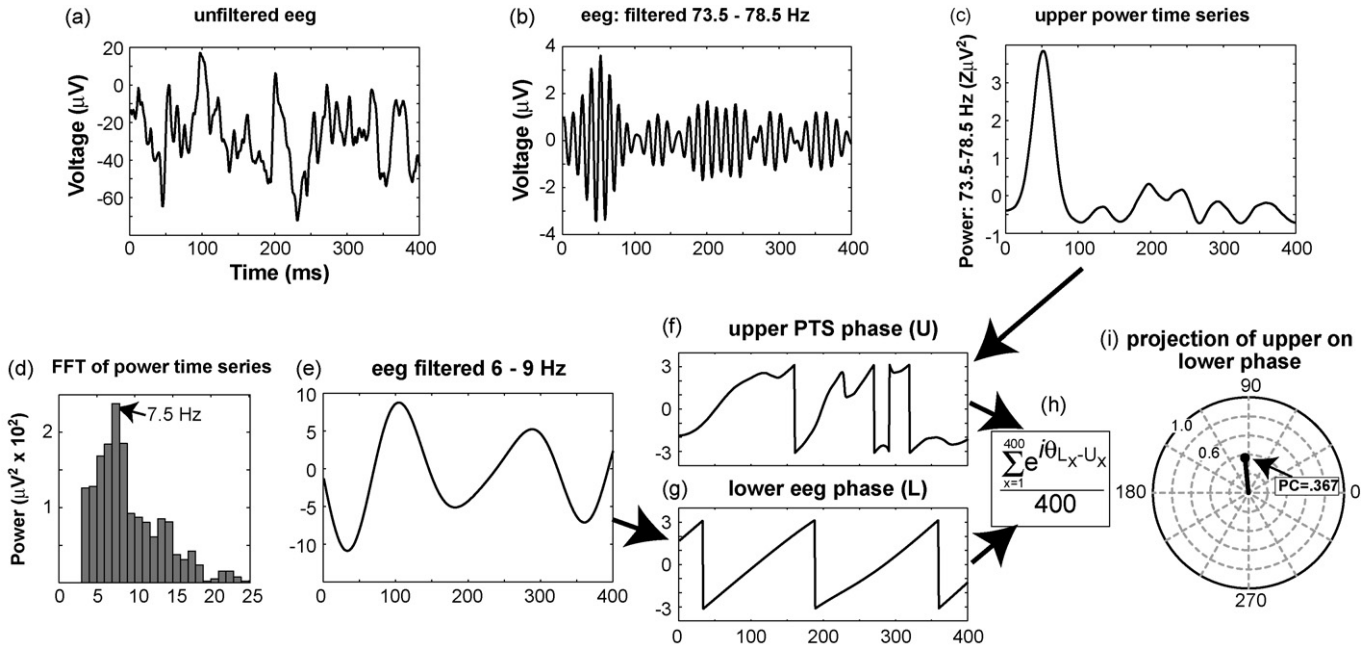

Fig. 1. Graphical overview of cross-frequency coupling method.

a priori chosen value above which one does not expect synchronization. The peak power component from the FFT therefore reflects the dominant frequency at which the upper frequency power time series oscillates. It is assumed that this is the synchronization frequency, and is selected by the analysis for further investigation. In this example, the peak is at 7.5 Hz (Fig. 1D). Note that a peak at 7.5 Hz does not necessitate that the 75 Hz oscillation be coupled with a 7.5 Hz oscillation. For example, if the phase of a 75 Hz oscillation were coupled with the phase of a 37.5 Hz oscillation (i.e., n:m coupling), but the 75 Hz power time series did not have a strong peak at 37.5 Hz, the present method might miss this coupling. Therefore, this step can be thought of as empirically identifying a likely coupling frequency, based solely on the proposition that a power time series will fluctuate at the frequency that modulates it.

At this point, upper and lower frequency bands have been identified at which transient cross-frequency coupling might occur. The third step is to extract the phase time series from both frequency bands, and compare them using standard phase coherence measures. For the upper frequency band, phases were extracted from the Hilbert transform of the power time series (phase = arctan(imag[$z(p(t))$]/real[$z(p(t))$])). Note that this phase time series does not reflect the phases of the 75 Hz oscillations, but rather the phase of the fluctuations in the power time series of the 75 Hz oscillations (Fig. 1F). The power time series should be normalized, de-trended, or mean-subtracted to have the DC-component removed; this ensures that phase values are not limited in range. For the lower frequency band, the EEG data are first band pass filtered, here using a 3 Hz window around the frequency identified in the previous step (thus, the EEG data are filtered from 6 to 9 Hz; Fig. 1E); the phase time series is then obtained from the angle of the Hilbert transform of the band-pass filtered signal (Fig. 1G). Again, one must filter a larger EEG time window to avoid edge-effect artifacts from contaminating the data. At this point, two phase times series have been obtained, one from the upper frequency band (75 Hz) that has been observed to contain 7.5 Hz oscillations, and one from the lower frequency band that was specifically filtered in this empirically identified frequency range (7.5 Hz). The synchronization between these two phase time series can be calculated using the phase coherence measure (synchronization index, SI; Fig. 1H):

$$\mathrm{SI} = \frac{1}{n} \times \sum_{t=1}^{n} \mathrm{e}^{\mathrm{i}[\phi_{\mathrm{l}t} - \phi_{\mathrm{u}t}]}$$

where n is the number of time points, $\phi_{\mathrm{u}t}$ is the phase value of the fluctuations in the upper frequency power time series at time point t, and $\phi_{\mathrm{l}t}$ is the phase value of the lower frequency band time series at time t. SI is a complex number, the magnitude of which, |SI| or SI_m, reflects the extent to which phases are synchronized. SI_m values vary between 0 and 1, with 0 indicating that phases are completely desynchronized, and 1 indicating that phase values are perfectly synchronized. When calculated across the window of time, each SI value reflects the extent to which the fluctuations in the power time series of the upper frequency band are phase-synchronized with oscillations in the lower frequency band across that window of time. If one takes the phase angle of SI instead of the magnitude, SI_p (arctan(imag[SI]/real[SI])) is the "preferred phase" of the synchronization—that is, the phase of the lower frequency at which coupling is maximal in that time window (Fig. 1I). In this approach, phase coherence outperforms a correlation measure because if the upper frequency power time series and lower frequency filtered EEG are tightly synchronized but phase-shifted by 90°, the correlation coefficient between the two signals will be close to zero; in contrast, they would exhibit significant phase coherence.

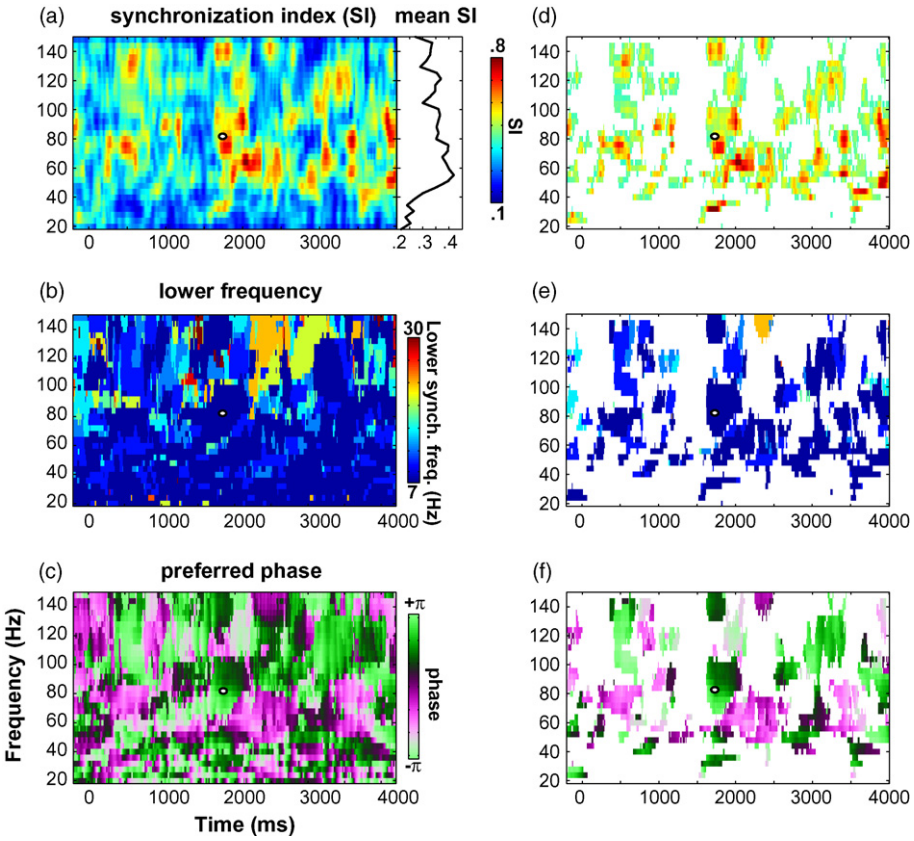

Fig. 2. Time–frequency maps show results from intracranially implanted electrode in the lateral temporal cortex of one patient. (a) Shows synchronization indices reflecting the extent to which the power time series of the frequencies listed on the *y*-axis are phase-synchronized with lower frequency band activity over time (*x*-axis), (b) shows the lower frequency bands empirically identified as being coupled with the power time series, (c) shows the preferred phase of the upper frequency power time series in the phase space of the lower frequency oscillation. (d–f) Same as (a–c) except only pixels that achieved $p < 0.01$ by a boot-strapping technique are displayed.

The previous procedure generates a single point in time–frequency space (in this example, the white circle in the graphs in Fig. 2). To generate a full map of cross-frequency coupling in time–frequency space, this three-step procedure is conducted repeatedly over moving windows of time and frequency. Here, this was conducted in overlapping windows, moving 10 ms in each iteration. The three outputs at each point in time–frequency space—SI, the lower frequency, preferred phase, can be plotted separately (Fig. 2A–C).

4. Statistical tests

Statistics can be conducted in one of several ways, for example via data-based bootstrapping techniques in order to determine the distance between the observed SI_m value and those expected by chance, or by transforming SI_m values via the Fisher *z*-transform and entering into a standard statistical software package such as SPSS. The former method is useful for determining whether cross-frequency coupling is greater than would be observed by chance; the latter method is useful for parametric statistics, for example, determining whether cross-frequency coupling differs over different periods of time or experimental conditions.

The boot-strapping technique is based on a comparison of the observed SI_m value to a distribution of SI_m values that was obtained by repeated random re-assignment of phase values from scrambled data. In this procedure, the phase time series obtained from the Hilbert transform of the upper frequency power time series is shifted in time by some random amount, and the SI_{mb} (b for bootstrapped) is calculated with the phase of the lower frequency phase time series, as described earlier. This procedure is repeated many times (here, 200 iterations) to create a distribution of SI_{mb} values; if the observed SI_m exceeds some percentage (say, 99%) of the SI_{mb} values, it is deemed statistically significant, and one may conclude that the synchronization at this time–frequency point likely did not arise by chance. In Fig. 2(D–F) only time–frequency points that achieved boot-strapped significance of $p < 0.01$ are displayed.

There are other methods for creating surrogate datasets useful for bootstrapping. For example, the upper frequency power time series could be decomposed into its power and phase components via the FFT ($m_f = A_f \times (\cos \varphi_f + i \times \sin \varphi_f)$, where A_f is the amplitude of power at frequency component *f*, and φ is the phase angle of frequency component *f*), the phase angles of each frequency bin ($\cos \varphi_f + i \times \sin \varphi_f$) are randomly shuffled, the signal is then reconstructed via inverse-FFT, and then the phase time series is extracted and the synchronization with the intact lower frequency signal is computed. Although this is a commonly used method for creating surrogate data, if the distribution of phases for the surrogate data is significantly different from that of the

actual upper frequency power time series, it is possible that this could affect the statistical tests. Because the former method uses the same distribution of phase values for the boot-strapping, it might be preferable in this case. Both boot-strapping methods were applied to the data shown in Fig. 2(D–F), and the thresholded results were similar.

For a standard statistical analysis, SI_m values should be Fisher z-transformed ($0.5 \times \log([1 + SI_m]/[1 - SI_m])$. This is because standard statistics assume that dependent variables are drawn from a normally distributed population of values; SI_m values violate this assumption because they have a range limited to [0, 1]. Fisher transformed values allow SI_m values to satisfy this assumption. From here, standard statistics can be used as appropriate, such as an ANOVA. It is recommended that SI_m values are averaged together in time–frequency windows (e.g., in steps of 500 ms and specified frequency bands like alpha, beta, lower gamma, upper gamma), because neighboring SI_m values will be correlated with each other. This method is useful for determining whether transient cross-frequency couplings change over time and/or over experimental condition. However, a non-uniform distribution of phases, if it differs systematically across time and/or condition, might also influence these results. In this case, one possibility is to use the boot-strapping method described earlier to transform that SI_m values to Z scores by comparing the distance of SI_m to the distribution of SI_{mb}: $Z_{tf} = (SI_m - \text{mean}(SI_{mb}))/\text{std}(SI_{mb})$, where Z_{tf} is the normalized synchronization index at time t and frequency f, and std is the standard deviation of distribution of SI_{mb} values. Z_{tf} is therefore an unbiased estimate of the distance of the away from the distribution of synchronization values expected under the null hypothesis of no synchronization; these values can then be used in parametric statistical tests.

Aside from these statistical tests, it might be useful to use the present analyses as an exploratory approach to determine where cross-frequency coupling exists in time and frequency. One could identify, based on visual inspection or other means, salient clusters in the results and conduct further analyses to test for other kinds of cross-frequency coupling (e.g., phase–amplitude coupling or n:m phase coupling), or test whether the observed coupling is specific to the lower frequency band identified.

5. Interpretation of results

From inspection of Fig. 2, it can be seen that significant cross-frequency coupling was observed in the gamma frequency range, especially around ~40–80 Hz. The lower frequency of this coupling was generally around 7–10 Hz (i.e., upper theta to lower alpha). This concentration of cross-frequency coupling in this range is interesting in light of previous research: gamma oscillations have been observed in several regions of the brain, and have been linked to cognitive and neural processes, including attention, perception, memory, and information processing (Steriade, 2006; Fries et al., 2007; Jensen et al., 2007). Furthermore, cross-frequency coupling has been observed in this frequency range, such that gamma oscillations increase during specific phases of theta in the hippocampus and in the neo-cortex (Chrobak and Buzsaki, 1998; Buzsaki and Draguhn, 2004; Jones and Wilson, 2005; Lakatos et al., 2005; Mormann et al., 2005; Canolty et al., 2006). Indeed, gamma power is generally maximal around troughs of theta, which is also consistent with what we found. Thus, our results are consistent with previous literature implicating gamma in cognitive processes, and in relating gamma power oscillations to theta waves.

6. Limitations and conclusions

Practically, this procedure is time- and processor-intensive. Down-sampling in time and frequency, or using parallel clustered computer networks to run analyses are ways to decrease computation time. Physiologically, it is generally assumed that upper frequencies are synchronized to the lower frequency, although the inverse could occur as well. Which frequency band – if any – is inducing modulations in the other frequency band is not addressed here. Other methods exist to estimate causality in time series data, including state space approaches (Osterhage et al., 2007) and lagged phase coherence measures; these measures could be incorporated into the present approach. Finally, cross-frequency coupling can manifest in many ways, and the method described here may not detect all of them. For example, as discussed earlier, if the upper power time series does not have a prominent oscillation component at the frequency with which it is actually coupled, it might not be measured using this method. The method presented here is particularly well-suited for transient and dynamic cross-frequency coupling. Given the flexibility of this method, and the relevance of the findings to previous research on gamma–theta interactions, this method appears appropriate for making brain–behavior links. One strength of this method is its flexibility: It could be modified to suit different purposes, for example, by incorporating estimates of causality. Another possible extension is to examine cross-channel coupling: The lower frequency activity could be taken from a separate electrode; this would then assess both cross-frequency and cross-channel coupling. In conclusion, a novel method for statistically identifying and assessing transient cross-frequency synchronization was presented. This method has some advantages over other currently used methods of cross-frequency synchronization, such as the ability to identify dynamic changes in synchronization over time and frequency. This approach might be especially useful in understanding how cross-frequency coupling relates to dynamic perceptual and cognitive processes that unfold over time.

Acknowledgements

I thank Juergen Fell and anonymous reviewers for comments on the manuscript, and Nikolai Axmacher and Thorsten Kranz for useful comments on the methods.

References

Bruns A. Fourier-, Hilbert- and wavelet-based signal analysis: are they really different approaches? J Neurosci Methods 2004;137:321–32.

Bruns A, Eckhorn R, Jokeit H, Ebner A. Amplitude envelope correlation detects coupling among incoherent brain signals. Neuroreport 2000;11:1509–14.

Buzsaki G, Draguhn A. Neuronal oscillations in cortical networks. Science 2004;304:1926–9.

Canolty RT, Edwards E, Dalal SS, Soltani M, Nagarajan SS, Kirsch HE, et al. High gamma power is phase-locked to theta oscillations in human neocortex. Science 2006;313:1626–8.

Chrobak JJ, Buzsaki G. Gamma oscillations in the entorhinal cortex of the freely behaving rat. J Neurosci 1998;18:388–98.

Delorme A, Makeig S. EEGLAB: an open source toolbox for analysis of single-trial EEG dynamics including independent component analysis. J Neurosci Methods 2004;134:9–21.

Demiralp T, Bayraktaroglu Z, Lenz D, Junge S, Busch NA, Maess B, et al. Gamma amplitudes are coupled to theta phase in human EEG during visual perception. Int J Psychophysiol 2007;64:24–30.

Fries P, Nikolic D, Singer W. The gamma cycle. Trends Neurosci 2007.

Jensen O, Colgin LL. Cross-frequency coupling between neuronal oscillations. Trends Cogn Sci 2007;11:267–9.

Jensen O, Kaiser J, Lachaux JP. Human gamma-frequency oscillations associated with attention and memory. Trends Neurosci 2007;30:317–24.

Jones MW, Wilson MA. Theta rhythms coordinate hippocampal-prefrontal interactions in a spatial memory task. PLoS Biol 2005;3:e402.

Lakatos P, Shah AS, Knuth KH, Ulbert I, Karmos G, Schroeder CE. An oscillatory hierarchy controlling neuronal excitability and stimulus processing in the auditory cortex. J Neurophysiol 2005;94:1904–11.

Le Van Quyen M, Foucher J, Lachaux J, Rodriguez E, Lutz A, Martinerie J, et al. Comparison of Hilbert transform and wavelet methods for the analysis of neuronal synchrony. J Neurosci Methods 2001;111:83–98.

Lisman J. The theta/gamma discrete phase code occurring during the hippocampal phase precession may be a more general brain coding scheme. Hippocampus 2005;15:913–22.

Mitra SK. Digital signal processing. 3rd ed. McGraw-Hill; 2001.

Mormann F, Fell J, Axmacher N, Weber B, Lehnertz K, Elger CE, et al. Phase/amplitude reset and theta–gamma interaction in the human medial temporal lobe during a continuous word recognition memory task. Hippocampus 2005;15:890–900.

Osterhage H, Mormann F, Wagner T, Lehnertz K. Measuring the directionality of coupling: phase versus state space dynamics and application to EEG time series. Int J Neural Syst 2007;17:139–48.

Palva JM, Palva S, Kaila K. Phase synchrony among neuronal oscillations in the human cortex. J Neurosci 2005;25:3962–72.

Quian Quiroga R, Kraskov A, Kreuz T, Grassberger P. Performance of different synchronization measures in real data: a case study on electroencephalographic signals. Phys Rev E Stat Nonlin Soft Matter Phys 2002;65:041903.

Schack B, Weiss S. Quantification of phase synchronization phenomena and their importance for verbal memory processes. Biol Cybern 2005;92:275–87.

Schack B, Klimesch W, Sauseng P. Phase synchronization between theta and upper alpha oscillations in a working memory task. Int J Psychophysiol 2005;57:105–14.

Steriade M. Grouping of brain rhythms in corticothalamic systems. Neuroscience 2006;137:1087–106.

Tass P, Rosenblum MG, Weule J, Kurths J, Pikovsky A, Volkmann J, et al. Detection of $n > m$ phase locking from noisy data: application to magnetoencephalography. Phys Rev Lett 1998;81:3291–4.

Varela F, Lachaux JP, Rodriguez E, Martinerie J. The brainweb: phase synchronization and large-scale integration. Nat Rev Neurosci 2001;2:229–39.